PHILOSOPHICAL TRANSACTIONS OF THE ROYAL SOCIETY A MATHEMATICAL, PHYSICAL & ENGINEERING SCIENCES

Strain and Anisotropy in Rocks [and Discussion]

D. S. Wood, G. Oertel, J. Singh, H. F. Bennett and D. H. Tarling

Phil. Trans. R. Soc. Lond. A 1976 **283**, 27-42
doi: 10.1098/rsta.1976.0067

Phil. Trans. R. Soc. Lond. A. **283**, 27–42 (1976) [27]
Printed in Great Britain

Strain and anisotropy in rocks

By D. S. Wood
Department of Geology, University of Illinois, Urbana, U.S.A.

G. Oertel
Department of Geology, University of California, Los Angeles, California, U.S.A.

J. Singh
Department of Geophysics and Planetary Physics, The University, Newcastle upon Tyne, England

and H. F. Bennett
Department of Geology, Michigan State University, East Lansing, Michigan, U.S.A.

[Plate 1]

The evaluation of finite strain in naturally deformed rocks is restricted by the limited occurrence of good natural strain indicators which are also homogeneous with respect to the matrix. This problem is overcome by establishing the relation between measured finite strain and those physical behaviour characteristics of rocks that are dependent upon the anisotropy resulting from deformation. Accordingly, the strain measured from natural indicators is calibrated against (*a*) degree of preferred orientation, (*b*) magnetic susceptibility anisotropy, and (*c*) seismic anisotropy. This will permit three approaches to be used independently for the evaluation of strain, provided that a minimal number of actual strains are available.

The relation between measured strain and the degree of preferred orientation of layer silicates as revealed by X-ray transmission goniometry is established for a group of fine grained tectonites of dominantly planar fabric which have an average deformation ellipsoid of form 1.6:1:0.26. The strains measured from the degree of preferred orientation are in remarkable agreement with those measured from natural strain indicators. The measured deformation ellipsoids for a wide range of strains are also compared to the correlative ellipsoids of magnetic susceptibility anisotropy. The axes of both sets of ellipsoids are coincidental and the shape relationship between deformation and magnetic susceptibility ellipsoids is established by linear regression. Finally, the anisotropy of seismic velocities is determined by measuring the pseudocompressional velocity and two orthogonally polarized pseudo shear wave velocities for each of a minimum of nine non-coplanar directions. The velocity surfaces thus obtained define an elastic or seismic velocity anisotropy ellipsoid, the axes of which are also precisely coincidental with those of the finite deformation ellipsoid. The influence of rock fabric upon seismic velocities is such that for a rock which has undergone a principal finite extension of 135 % and a finite shortening of 65 %, the difference of compressional and shear wave velocities between these two directions is in the ratio 1.26:1 for *P* waves and 1.33:1 for *S* waves.

Introduction

The Cambrian Slate Belt of Wales provides an ideal opportunity for making a first attempt to apply four independent methods to the investigation of strain in highly anisotropic rocks characterized by slaty cleavage. Lower Cambrian slates, approximately 1 km in vertical thickness occur in a strongly deformed zone that is 24 km in length and up to $2\frac{1}{2}$ km in width,

marking the northwestern margin of the Welsh Lower Palaeozoic Basin. Caledonian deformation produced a uniformly well-developed slaty cleavage parallel to the axial surfaces of folds and the strain associated with this deformation may be measured from ellipsoidal iron-reduction bodies (figure 1, plate 1) which occur at several stratigraphic horizons in the Lower Cambrian sequence.

These natural strain indicators are perfect triaxial ellipsoids which have their principal plane parallel to the plane of slaty cleavage, irrespective of varying angular relations between the cleavage and the primary sedimentary layering. From a geometric consideration, it can be demonstrated that the indicators were initially spherical. The indicators may be shown to be pre-deformational in age, in view of the fact that the reduction bodies are obliterated by the contact metamorphic effect of Ordovician dolerite dykes which were themselves subjected to the deformation.

The indicators were first described as 'reduction spots' by Sorby (1855). They are ellipsoidal bodies in which the total iron content of the rock is drastically depleted rather than being in a different oxidation state compared to the enclosing rock. The ellipsoids are the result of iron diffusion from point sources that are small compared to the volume of each ellipsoidal body. As such, they are at one end of a development spectrum, the opposite end of which consists of continuous planar zones of iron depletion along the primary sedimentary layering. The iron which has been depleted was mainly fine-grained haematite and its removal permits the otherwise masked pale green colour of chlorite to contrast with the purple and red colours of the non-depleted bulk of the rock. Iron migration is believed to have been dependent upon the presence of traces of organic material which gave rise to locally reducing conditions and to the formation of organic acids. The resulting potential would have given rise to a concentration cell effect. These conditions allowed complexing or reduction of ferric iron, possibly to a divalent iron gel which, under the influence of the potential, migrated in solution to sites where the conditions were inadequate to have had any effect upon existing haematite and where the transported iron could be precipitated in its original form. All of the ellipsoidal iron-reduction bodies have clearly defined precipitation rims where iron ranges from 8.5 to 14 % by mass.

Strain from natural strain indicators

The reduction bodies are initially observed as ellipses upon natural cleavage faces of the rock. They are polished parallel to the cleavage and cut in the two directions perpendicular to the cleavage that are also parallel to the axes of the observed ellipse. This procedure serves to ascertain that more than half of the short dimension is present and to verify that the principal plane of the ellipsoid is indeed parallel to the cleavage. The process of polishing enables serial axial ratios to be measured and their constancy demonstrates the true triaxial nature of the ellipsoids. The individual cutting of the ellipsoids (Tullis & Wood 1975) is followed by polishing precisely to the three symmetry planes. This permits accurate measurement of two half-axes and one complete axis and also ascertains that the nucleus of the ellipsoid is small compared to its volume.

Principal strains are obtained by comparing the axial dimensions with the diameter of equivalent volume spheres in each case. This ignores possible volume changes that may have occurred during deformation. The consequences of neglecting volume change have been discussed by Ramsay & Wood (1973). They may well mean that observed shortening strains are lower, and observed extensional strains higher than the actual strains. However, the rocks in question

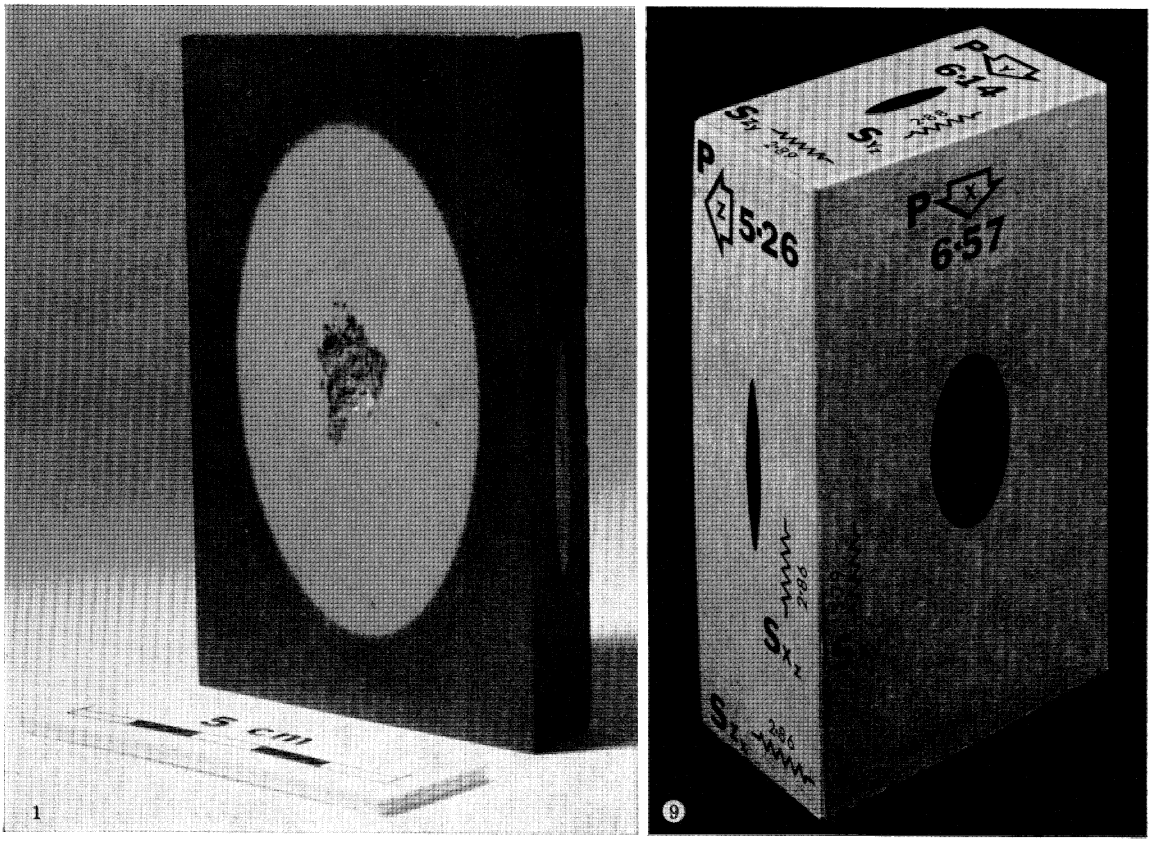

FIGURE 1. Ellipsoidal iron-reduction bodies from the Lower Cambrian slates at Penrhyn Quarry, Bethesda, North Wales. Specimen cut parallel and perpendicular to the cleavage showing the principal plane (X–Y) and the plane X–Z of the deformation ellipsoid.

FIGURE 9. Schematic block representation of the 9 seismic velocities for the principal strain directions X, Y and Z of slate with deformation ellipsoid of axial ratio 1.63:1:0.26 from Penrhyn Quarry, Bethesda, North Wales. Arrows indicate propagation direction of P waves. Propagation and vibration directions of S waves indicated. Velocities are in kilometres per second.

(*Facing p.* 28)

PHILOSOPHICAL TRANSACTIONS OF THE ROYAL SOCIETY A MATHEMATICAL, PHYSICAL & ENGINEERING SCIENCES

must have been lithified and in an advanced diagenetic state at the time of deformation since they had already undergone fracturing during the emplacement of Middle Ordovician dolerite dyke swarms prior to the end-Silurian deformation (Wood 1974, pp. 395–7). If the progression from lithified mudstone to slate involved a volume loss of no more than 20 % (Ramsay & Wood 1973, p. 267), comparison of the deformation ellipsoid with an equivalent volume sphere would involve only minimal errors in view of the small change in sphere diameter.

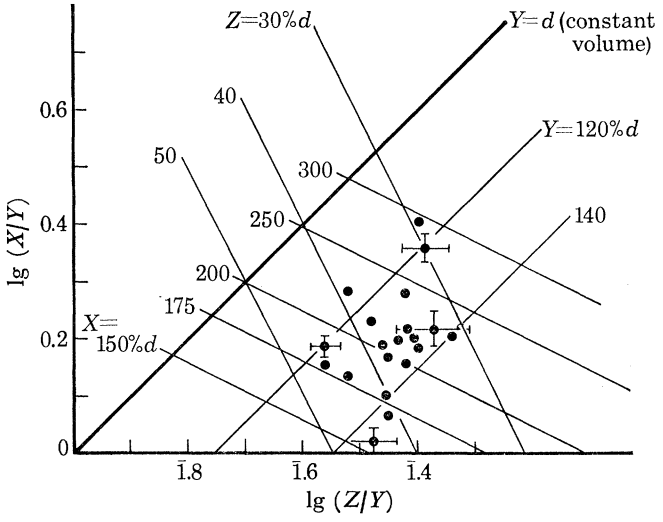

FIGURE 2. Logarithmic deformation plot showing average values of 30 deformation ellipsoids measured at 20 localities in the Cambrian Slate Belt of Wales. Standard deviations are indicated for four representative localities.

Accordingly, the measured strains are plotted on the logarithmic constant volume deformation plot (Wood 1974, figure 1). The three axes of the deformation ellipsoid X, Y, Z are related to the principal strains as $1+e_1$, $1+e_2$, $1+e_3$, where e_1, e_2 and e_3 are the principal extensions. The ratio $(1+e_1)/(1+e_2)$ is plotted as the ordinate (X/Y); and the ratio $(1+e_3)/(1+e_2)$ is plotted as the abcissa (Z/Y). The average deformation ellipsoids from complete measurement of 30 deformation ellipsoids at each of 21 localities are plotted in figure 2. The straight lines of equal dimensional change on this plot show that the average principal finite strains are approximately such that compared to the equivalent sphere diameter (d); $X = 230\,\%d\,(e_1 = 1.30)$; $Y = 130\,\%d\,(e_2 = 0.30)$; and $Z = 35\,\%d\,(e_3 = -0.65)$. All ellipsoids fall in the field of apparent flattening of the deformation plot (Ramsay & Wood 1973). Most ellipsoids are centrally situated, although some virtually plot along the abscissa as oblate spheroids. The largest measured finite extensional strains involve a trebling of dimension $(X = 300\,\%d)$ and the largest finite shortening strains are 70 % $(Z = 28\,\%d)$. For a representative number of the localities for which the average deformation ellipsoid is plotted, the standard deviations are indicated on figure 2. The variations in strain exhibited in the Cambrian Slate Belt of Wales are considerable and the close relationship between strain variation and large scale structure has been demonstrated (Wood 1974, pp. 382–4). The large scale fold structures with which the cleavage is associated show major culminations and depressions along their axes. The plunge culminations are the result of greater vertical extensional strains in the axial plane cleavage dependent upon greater finite shortening across the cleavage, whereas plunge depressions are characterized by smaller finite shortening. Thus shortenings of 55 % $(Z=45\,\%d)$ are typical of

plunge depressions and shortenings of 70 % ($Z = 30\ \%d$) are common in the plunge culmination zones where sub-vertical tectonic extension has usually resulted in a greater than doubling of original vertical thickness. The strain variations which can thus be measured and related to large scale geological structure should also be capable of being qualitatively and quantitatively related to other physical measurements of anisotropy.

Strain from preferred orientation

The only satisfactory method for the investigation of preferred orientation in fine-grained aggregates is provided by X-ray analysis. The application of X-ray photographic methods to problems of preferred mineral orientation in deformed rocks dates from the work of Sander & Sachs (1930) and has achieved greater precision with the more refined methods of Wenk (1963, 1965) and Starkey (1964). The first quantitative measurements of preferred orientation of platy elements were obtained by Means & Paterson (1966) from experimentally deformed aggregates. X-ray texture or pole-figure goniometry has been applied to the investigation of preferred orientation of phyllosilicates in natural slates (Oertel 1970; Tullis & Wood 1972, 1975; Oertel & Wood 1974) and the degree of preferred orientation compared to the finite strain measurement obtained from natural indicators.

The preferred orientation of muscovite was measured with the X-ray texture goniometer following the method of Baker, Wenk & Christie (1969), as modified by Oertel (1970). X-rays are transmitted through two mutually orthogonal sections from each specimen. The sections are most conveniently both taken approximately at right angles to the slaty cleavage. If the cleavage contains any lineation or 'grain', the sections are taken parallel and orthogonal to this lineation. No particular orientation of sections is necessary if a third orthogonal section is added. Sections are ground to a thickness of 100 μm. For an individual goniometer run, the X-ray detector is held at a constant angle to the primary beam, so that only crystallographic planes of a given spacing are observed. In the present study, the spacing was 1.002 nm for muscovite (002) planes. The section is then rotated and tilted so that the intensity of diffracted X-rays is scanned successively for different attitudes of the investigated crystallographic plane.

The background intensity is subtracted from the observed intensities; net intensities from the two or three orthogonal sections are combined, and the combined intensity is normalized by expressing it in multiples of the mean intensity for the specimen. The result is a fabric diagram like that of figure 3. The technical procedure has been described in greater detail by Oertel & Curtis (1972).

Strains can be inferred from the orientation of platy particles in a rock provided that such particles were initially randomly oriented and if the strain was homogeneous, having affected both particles and matrix equally (March 1932; Owens 1973). In practice the latter assumption can be confidently relaxed (Tullis 1971, pp. 193–202). The principal strains e_i at constant volume are related to principal normalized densities (ρ_i) of poles on the plane surfaces of platy particles by:

$$e_i = \rho_i^{-\frac{1}{3}} - 1, \tag{1}$$

where densities may be replaced by normalized X-ray intensities. The strain so measured is the total strain from the time when the particles were at random to the time of observation, including any strain due to compaction of sedimentary materials, but without consideration of volume change.

The magnitude and orientation of the maximum intensity are easily determined. If the intensity distribution has orthorhombic symmetry, which is usually the case if the fabric is spatially homogeneous throughout the sample, then the three principal planes and directions of the intensity distribution can be determined by inspecting the fabric diagram for orthogonal planes of mirror symmetry. The positions of the points ρ_1 and ρ_2 on figure 3 were thus determined. However, the magnitudes of the intensities at the two lesser principal intensities are generally so small that they cannot be estimated directly with sufficient precision for a useful strain determination. Rather, these magnitudes must be estimated by the following method.

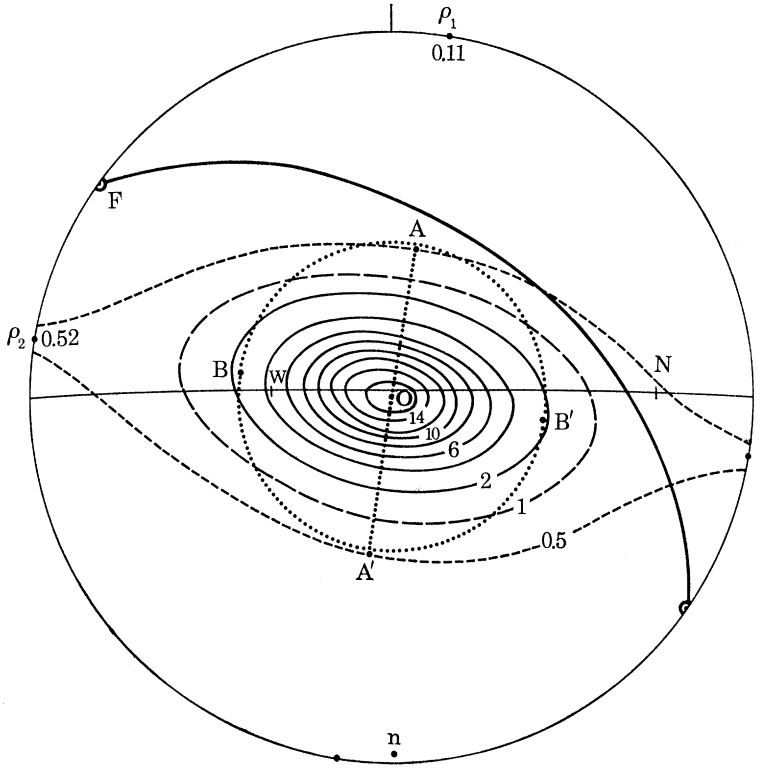

FIGURE 3. Equal-area projection of intensity distribution of X-rays diffracted by basal plane of muscovite in slate sample from Penrhyn Quarry to illustrate method of determining orientations and magnitudes of principal intensities. Fundamental circle: trace of slaty cleavage. Thin line: trace of horizontal plane, with N and W cardinal directions. Heavy line: trace of bedding, with F as fold axis defined by intersection with cleavage. n, nadir. Contours: intensities of diffracted X-rays, plotted on poles of diffracting planes, in multiples of random intensity and intervals of twice random. Long dashed and short dashed contours: same at reduced intervals. $\rho_1 = 0.11$: least principal density (corresponding to principal extensive strain). $\rho_2 = 0.52$: intermediate principal density. O: pole of cleavage, locus of $\rho_3 = 17.22$. Dotted straight line A A′: trace of principal plane of density distrubution through θ and ρ_1, with intercepts by the 0.5 random contour. Dotted circle: small circle about O at distance of mean between OA and OA′. B, B′: intercepts of small circle with trace of principal plane through O and ρ^2. Intensities at B, B′ are 2.5, 2.2 times-random.

It may be assumed that the unknown ratio of the two principal intensities at 90° from the maximum (i.e. at the periphery of figure 3), is little different from the ratio of the two known intensities, also at equal distance from the maximum and also in the principal planes, in the region of the lowest contour that might be considered reliable. The trace of the principal plane containing maximum and minimum intensity on figure 3 is intercepted by the 0.5 times-random contour at points A and A′. With ideal symmetry, the angular distances of these points

from the maximum (O) should be identical. The observed distances are 34° and 36°. Taking the mean distance as 35° (dotted circle ABA′B′), it is found that the 35° small circle about O intercepts the other principal plane of the intensity distribution at B and B′. The observed intensity at B (ρ_B) is 2.5 times-random, and that at B′ ($\rho_{B'}$) is 2.2 times-random. This constitutes a minor violation of the required symmetry. Taking $\bar{\rho}_B = 2.35$ times-random, the mean of intensities at B and B′, as the true maximum intensity along the 35° small circle and the mean minimum at A and A′ ($\bar{\rho}_A$) as 0.5 times-random, the ratio of the mean maximum over mean minimum is found to be 4.7. If this is taken to be also the ratio of ρ_2/ρ_1, then there is only one set of principal intensities which, including the observed intensity for ρ_3 of 17.22, obeys the relation:

$$\rho_1\rho_2\rho_3 = 1. \tag{2}$$

Equation (2) is deduced from equation (1) for the case $(1+e_1)(1+e_2)(1+e_3) = 1$, thus for constancy of volume. The unique set of principal intensities for the example shown in figure 3 is $[\rho_i] = [0.111\ 0.52\ 17.22]$ and this means, according to equation (1), that the principal strains are,

$$[e_i] = [1.08 \quad 0.24 \quad -0.61]. \tag{3}$$

The stereoplot (figure 3) is of a specimen for which the deformation ellipsoid from natural indicators has the form 1.63:1:0.26, being a reasonable average for the Cambrian Slate Belt. The principal finite strains obtained for this ellipsoid from the deformation plot (figure 2) are as follows:

$$X = 220\ \%d\ (e_1 = 1.20);\ Y = 133\ \%d\ (e_2 = 0.33);\ Z = 35\ \%d\ (e_3 = -0.65),$$

whereas the strains measured from the preferred orientation by the above method are:

$$X = 208\ \%d\ (e_1 = 1.08);\ Y = 124\ \%d\ (e_2 = 0.24);\ Z = 39\ \%d\ (e_3 = -0.61).$$

The lower strain values obtained from the preferred orientation compared to those obtained from the natural indicators are compatible with results from the same area obtained by Tullis & Wood (1972, 1975). The latter considered only the principal finite shortening strain and found that for rocks which had undergone shortenings of 63 %, 66 % and 68 %, the measured maximum pole concentrations for mica (002) were precisely normal to the slaty cleavage, with values of 16.3, 17.9 and 18.3 times-random respectively. These concentrations are lower than the concentrations predicted according to the model of March (1932) for the measured strains which are, respectively, 20.6, 25.6, and 31.6 times-random. Accordingly, the finite shortening obtained from the measured preferred orientations is less than that indicated by the natural strain indicators.

In order satisfactorily to compare strains obtained by both methods, the procedure outlined above has been applied to some 40 samples from the Cambrian Slate Belt. The results are shown on the deformation plot, figure 4. The range of strains is comparable with the range obtained from natural strain indicators (figure 2). However, the strains obtained from preferred orientation are again generally lower. Whereas the average deformation ellipsoid obtained for the Cambrian Slate Belt from natural indicators has the form 1.6:1:0.26, that obtained from preferred orientation data has the form 1.5:1:0.32. The comparative average principal strains obtained by both methods are as follows:

(strain indicators) $X = 220\ \%d\ (e_1 = 1.20);\ Y = 134\ \%d\ (e_2 = 0.34);\ Z = 35\ \%d\ (e_3 = -0.65)$

(preferred orientation) $X = 191\ \%d\ (e_1 = 0.91);$

$Y = 128\ \%d\ (e_2 = 0.28);\ Z = 40\ \%d\ (e = -0.60).$

PHILOSOPHICAL TRANSACTIONS OF THE ROYAL SOCIETY A MATHEMATICAL, PHYSICAL & ENGINEERING SCIENCES

These twofold strain data may be more specifically compared in figure 5 where average deformation ellipsoids obtained from natural indicators at ten localities are plotted together with the deformation ellipsoids obtained from the preferred orientations at the same localities. The close agreement between the results from these two independent methods is encouraging. It demonstrates that, for the highly anisotropic deformed rocks of the Welsh Cambrian Slate Belt, X-ray goniometer evaluation of preferred orientation is a valuable method of strain measurement.

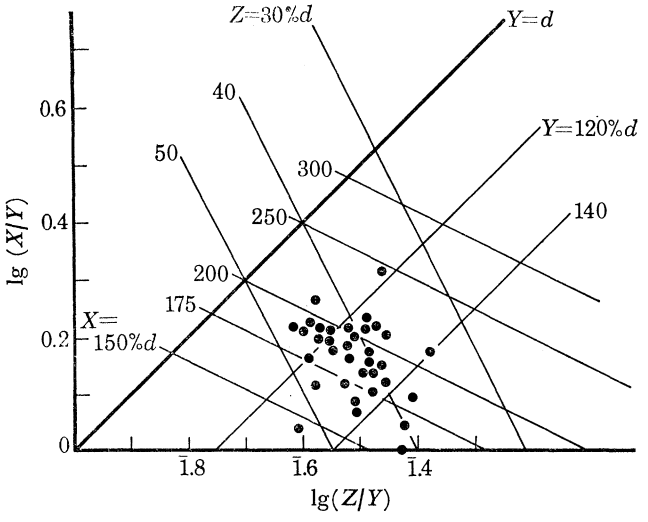

FIGURE 4. Logarithmic deformation plot showing deformation ellipsoids derived from principal strains obtained by preferred orientation measurement at 40 localities in the Cambrian Slate Belt of Wales.

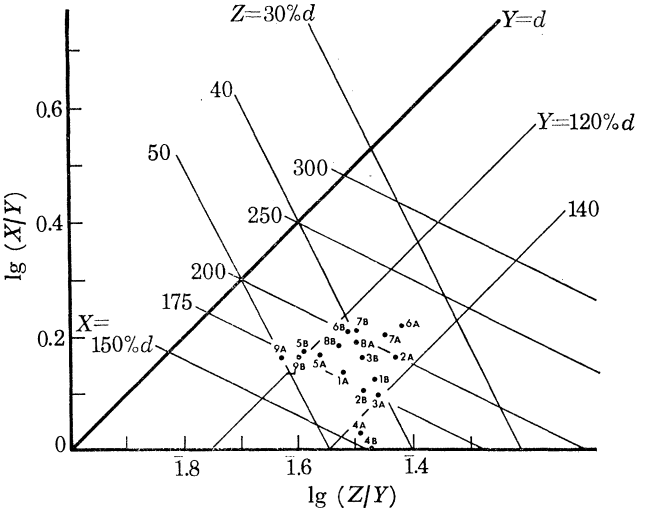

FIGURE 5. Logarithmic deformation plot showing correlative deformation ellipsoids obtained (A) by direct measurement of natural strain indicators and (B) calculated from preferred orientation measurement at 9 localities in the Cambrian Slate Belt of Wales.

Magnetic susceptibility anisotropy and strain

The magnetic anisotropy of magnetic mineral grains is attributable to one or both of two sources: shape effect anisotropy; and magnetocrystalline anisotropy. Shape effect anisotropy is important in high susceptibility cubic minerals such as magnetite, where the demagnetizing factors of the grains are highly sensitive to deformation and where small-scale strains produce a net anisotropy in the susceptibility of the rock. Magnetocrystalline anisotropy results from the net alignment of the easy magnetic axes of the lower susceptibility minerals of lower symmetry such as haematite and pyrrhotite, both of which have an easy magnetic basal plane and a hard axis along the *c*-axis of the crystal.

The suggestion that the use of magnetic fabric could be a valuable tool in petrofabric anlaysis was first made by Graham (1954). Until recently the measurement of magnetic anisotropy has been both tedious and imprecise. The development of faster techniques, which use a special head for the Digico magnetometer (Molyneux 1971), offers a routine tool for either local detailed studies or large-scale investigations (Singh, Sanderson & Tarling 1975). Although various studies have been carried out to determine the anisotropy of granites, slates and other rocks, there have been no detailed studies which test this technique independently against accurately known strain measurements.

Preliminary examination of the magnetic susceptibility anisotropy in various Welsh slates was undertaken by Fuller (1960, 1963, 1964). There has, as yet, been no attempt to relate the magnitude of magnetic susceptibility anisotropy to the finite strains of these rocks, although Fuller (1964, pp. 371–2) noted that the axes of the ellipsoid of magnetic susceptibility for the Cambrian slates of North Wales were parallel to those of the natural strain indicators, with the maximum susceptibility being parallel to the long dimension of the deformation ellipsoid.

The mineral responsible for the magnetic susceptibility anisotropy in the Cambrian slates of North Wales has been determined by X-ray diffraction and Curie point determinations as haematite. Unstrained crystalline haematite exhibits triaxial anisotropy in its basal plane. Anderson *et al.* (1954), Kumagai *et al.* (1955), Tasaki & Iida (1963), and Porath (1968) showed that compression in the basal plane of haematite crystals produces a strong basal plane anisotropy with uniaxial, biaxial and triaxial components. As would be expected for linear compression, the uniaxial terms are dominant. This stress induced anisotropy in haematite has been confirmed by ferromagnetic resonance experiments (Mizushima & Iida 1966).

Haematite occurs in slates as fine flakes or plates whose planes coincide with the crystallographic basal planes. Thus the susceptibility anisotropy in the Welsh Cambrian slates can be accounted for by the rotation of these grains to lie in the strongly developed cleavage, giving rise to the hard axis direction parallel to the sub-horizontal pole to the slaty cleavage. In the basal planes, the compaction due to adjacent grains gives rise to a maximum axis in the vertical direction and a minimum axis, corresponding to the total susceptibility ellipsoid intermediate axis, in the horizontal direction.

The present work concerns 31 randomly selected sites in the Cambrian Slate Belt, each site consisting of six separately oriented cores, 2.5 cm in diameter and approximately 8 cm in length. Measurements are carried out using a modified computer-linked slow spinner magnetometer (Molyneux 1971) in which the core is spun about three mutually perpendicular axes. The magneto meter unit calculates the orientation and magnitude of maximum, intermediate and minimum axes of the susceptibility ellipsoid with respect to the fiducal mark. The magnitude

measured is not the absolute magnitude along the axis but is the difference between the total susceptibility in a principal axis direction and the susceptibility along the axis of the core.

$$M_{i,j,k} = \chi_{i,j,k} - \chi_{\text{axial}}$$

where i, j and k represent the three principal directions. The χ_{axial} is measured on a standard susceptibility bridge (Collinson, Molyneux & Stone 1973), and hence the three absolute susceptibilities can be determined. Repeated measurements were found to give extremely reproducible results, both in the magnitude and orientation of the susceptibility ellipsoid. The results from different individual specimens at the same site also showed close correspondence and Fisher statistics (Fisher 1953) applied to axial orientations gave α_{95} less than 10°. The great advantage of the method is its speed and precision.

The total susceptibility of a rock can be represented as an ellipsoid with three mutually perpendicular axes χ_{maximum}; $\chi_{\text{intermediate}}$; χ_{minimum}. In the case of an isotropic material $\chi_{\text{max}} = \chi_{\text{int}} = \chi_{\text{min}}$. In magnetic fabric analysis, the ratios of the principal axes are used to definine the fabric. The ratios P_1, P_2 and P_3 are defined as:

$$P_1 = \chi_{\text{max}}/\chi_{\text{int}} = \text{lineation } (L),$$

$$P_2 = \chi_{\text{max}}/\chi_{\text{min}} = \text{'anisotropy factor'},$$

$$P_3 = \chi_{\text{int}}/\chi_{\text{min}} = \text{foliation } (F).$$

The lineation (L) is the intensity of linear parallel orientation of the ferromagnetic minerals in the rock and foliation (F) is the intensity of planar parallel orientation of the ferrogmagnetic minerals. The ratio $P_3/P_1 = E$, the eccentricity of the susceptibility ellipsoid. If $E > 1$, then the susceptibility ellipsoid is oblate and the magnetic foliation is more developed than the lineation and, conversely, if $E < 1$, then the susceptibility ellipsoid is prolate and the magnetic lineation is dominant.

The overall susceptibility ellipsoid at all sites was found to be oblate with typical values of $E = 1.10$ (table 1). For the majority of sites the anisotropy factor, P_2, lies between 1.15 and 1.25 with an average value of 1.21. P_1 has an average value of 1.08 and P_3 has an average value of 1.16. Following the analogy of the standard deformation plot, P_1 values are plotted against P_3 values on figure 6 from which the oblate nature of all the magnetic susceptibility ellipsoids is apparent. Thus the susceptibility ellipsoid has the same general form as the deformation ellipsoid.

Of the 31 sites considered in this study, 22 show an essentially vertical maximum-intermediate susceptibility plane which coincides with the slaty cleavage. The susceptibility maximum axes align sub-vertically and the susceptibility intermediate axes are sub-horizontal. The susceptibility minimum axes are normal to the plane of cleavage. For these 22 sites, the axes of the magnetic susceptibility ellipsoid are perfectly coincidental with the three principal strain directions. For the remaining 9 sites (nos. 11, 12, 13, 15, 16, 19, 20, 21 and 22 on tables 1 and 2) the maximum axes are also sub-vertical, but the directions of the intermediate and minimum axes appear to have been interchanged. There is nothing exceptional about the P and E values for these sites and there is no readily apparent explanation for this interesting anomaly which is under further investigation.

In order to compare the magnetic fabric data directly with strain data, orthogonal sections have been prepared from the actual samples used in the susceptibility examination. The strains measured from the preferred orientations in these samples have been reduced to axial data for

PHILOSOPHICAL TRANSACTIONS OF THE ROYAL SOCIETY A MATHEMATICAL, PHYSICAL & ENGINEERING SCIENCES

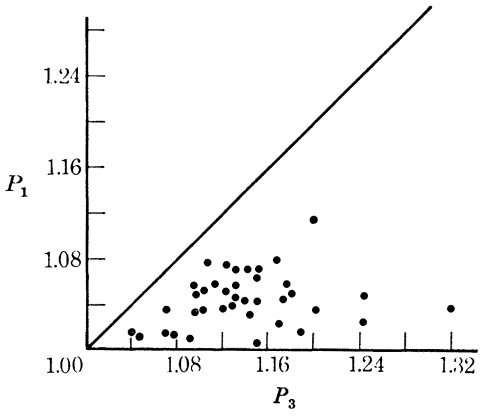

FIGURE 6. Plot of magnetic lineation (P_1) against magnetic foliation (P_3) for 31 localities in the Cambrian Slate Belt of Wales.

TABLE 1. AXIAL DATA FOR DEFORMATION ELLIPSOIDS AND MAGNETIC SUSCEPTIBILITY ELLIPSOIDS IN THE CAMBRIAN SLATE BELT OF WALES

no.	X/Y	X/Z	Y/Z	Y^2/XZ	P_1	P_2	P_3	'E'	grid reference (SH)	
1	1.35	3.50	2.58	1.91	1.063	1.217	1.146	1.078	630	692
2	1.26	2.81	2.24	1.78	1.058	1.177	1.113	1.052	631	693
3	1.30	4.05	3.12	2.40	1.035	1.366	1.321	1.277	632	689
4	1.60	4.34	2.73	1.71	1.077	1.192	1.107	1.029	623	655
5	1.26	3.49	2.77	2.19	1.080	1.262	1.168	1.082	623	653
6	1.51	3.83	2.53	1.67	1.117	1.350	1.206	1.079	624	651
7	1.50	3.79	2.53	1.69	1.056	1.195	1.130	1.070	622	650
8	1.64	4.69	2.86	1.74	1.006	1.158	1.151	1.144	602	627
9	1.59	4.34	2.73	1.71	1.029	1.177	1.144	1.112	603	627
10	1.44	4.11	2.86	1.99	1.059	1.246	1.177	1.111	592	611
11	1.40	3.78	2.70	1.92	1.074	1.230	1.458	1.067	597	608
12	1.44	3.74	2.60	1.80	1.053	1.177	1.117	1.061	597	597
13	1.17	2.65	2.27	1.95	1.009	1.097	1.087	1.077	562	601
14	1.15	2.09	1.83	1.60	1.034	1.108	1.071	1.036	563	601
15	1.17	2.74	2.33	1.99	1.069	1.206	1.129	1.059	539	584
16	1.42	3.27	2.31	1.63	1.051	1.180	1.123	1.068	530	569
17	1.26	3.18	2.52	2.00	1.034	1.244	1.203	1.163	528	570
18	1.26	3.73	2.96	2.34	1.050	1.242	1.183	1.127	518	561
19	1.53	4.25	2.77	1.81	1.069	1.214	1.136	1.062	517	560
20	1.06	3.42	3.22	3.03	1.024	1.274	1.244	1.215	501	540
21	1.34	4.12	3.07	2.29	1.047	1.311	1.252	1.196	505	535
22	1.00	2.67	2.67	2.67	1.017	1.209	1.189	1.170	510	553
23	1.20	3.10	2.58	2.15	1.042	1.186	1.139	1.093	574	608
24	1.46	3.06	2.09	1.43	1.049	1.155	1.100	1.049	587	601
25	1.32	3.44	2.60	1.97	1.041	1.174	1.129	1.085	552	600
26	1.41	4.33	3.07	2.18	1.043	1.224	1.174	1.126	538	584
27	1.55	3.85	2.49	1.61	1.034	1.124	1.087	1.051	519	561
28	1.26	3.27	2.59	2.06	1.034	1.124	1.087	1.051	517	559
29	1.28	2.85	2.22	1.73	1.014	1.087	1.073	1.058	515	549
30	1.73	5.20	3.00	1.73	1.067	1.382	1.288	1.203	491	522
31	1.71	5.36	3.13	1.83	1.023	1.196	1.169	1.142	588	595

PHILOSOPHICAL TRANSACTIONS OF THE ROYAL SOCIETY A MATHEMATICAL, PHYSICAL & ENGINEERING SCIENCES

the deformation ellipsoids at each site (table 1). This serves to facilitate comparison of the correlative data: (X/Y with P_1); (X/Z with P_2); (Y/Z with P_3); and (Y^2/XZ with E).

Initially we chose to compare the ellipticity factor (E) with the ratio Y^2/XZ of the deformation ellipsoid (figure 7). When the method of least squares is applied, the two sets of data are found to be related by the expression:

$$E_{\text{mag}} = 0.880 \pm 0.05 + (0.114 \pm 0.025)\ Y^2/XZ.$$

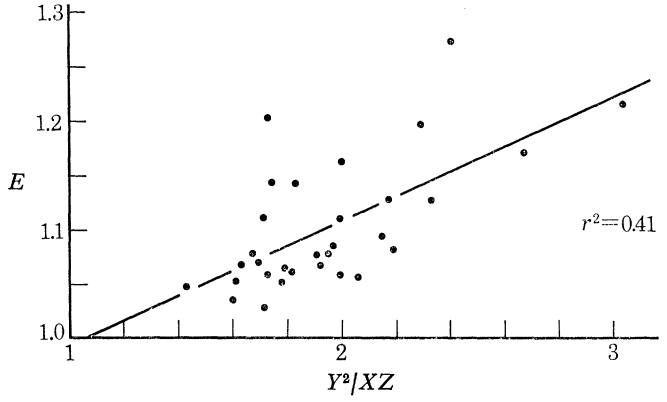

FIGURE 7. Plot of the magnetic susceptibility ellipsoid eccentricity (E) against the correlative term Y^2/XZ of the deformation ellipsoid for 31 localities in the Cambrian Slate Belt of Wales. $E_{\text{mag}} = 0.880 \pm 0.05 + (0.114 \pm 0.025)\ Y^2/XZ$.

The correlation coefficient for the data of figure 7 is 0.41. The relation derived does not give a satisfactory correlation between magnetic anisotropy and strain anisotropy for the samples sites as a whole since, for a good fit, the intercept should ideally be zero and the slope should show very little error. Similarly a plot of P_2 against X/Z gave the relation:

$$P_2 = 1.044 \pm 0.060 + (0.045 \pm 0.016)\ X/Z.$$

These correlations suggest that the relations between the two fabric parameters are not linear. Thus it was decided to determine a correlation between the actual deviations from the isotropic state for the respective magnetic and strain axes. Accordingly, the natural strains

$$N_i = \ln(\epsilon_i + 1)$$

were computed from the principal strains $\epsilon_i = (l_i - l_0)/l_0$. Similarly, the natural normalized susceptibilities $M_i = \ln(D_i + 1)$ were computed from the principal susceptibility deviators $D_i = (\chi_i - \chi_0)/\chi_0$ (table 2). A least squares straight line fit of M_i against N_i gave a more satisfactory result (figure 8). Since magnetic data was available for six samples at each locality, each point of the comparison was weighted with a weighting factor equal to $1/\sigma^2_{M_i}$ (table 2).

The relation between M_i and N_i was found to be:

$$M_i = 0.001 \pm 0.003 + (0.145 \pm 0.005)\ N_i,$$

with a correlation coefficient (r) of 0.973. In this case it is found that the intercept lies within a fraction of one standard deviation from zero and the slope error is under 3 %.

The linear correlation obtained can be treated as a calibration graph, thereby enabling magnetic susceptibility anisotropy to be translated directly into strain anisotropy. From this initial correlation, relations between more fundamental parameters may be determined. For

example, assuming the intercept on figure 8 to be zero, then the relation for the rocks in question may be rewritten as $(\chi_i/\chi_0) = (l_i/l_0)^{0.145}$
From this, the following can be derived:

$$P_1 = (X/Y)^{0.145},$$
$$P_2 = (X/Z)^{0.145},$$
$$P_3 = (Y/Z)^{0.145},$$
$$E = (Y^2/XZ)^{0.145}.$$

TABLE 2. PRINCIPAL NORMALIZED 'NATURAL' SUSCEPTIBILITIES, $(M_i \pm \sigma_{M_i})$, COMPARED WITH NATURAL STRAINS, (N_i), MEASURED BY PREFERRED ORIENTATION

no.	N_1	M_1	σ_{M_1}	N_2	M_2	σ_{M_2}	N_3	M_3	σ_{M_3}
1	0.52	0.086	0.037	0.21	0.025	0.037	0.73	0.110	0.039
2	0.42	0.073	0.025	0.19	0.017	0.025	0.61	0.090	0.024
3	0.55	0.101	0.037	0.29	0.067	0.038	0.85	0.168	0.068
4	0.64	0.084	0.036	0.18	0.009	0.031	0.83	0.093	0.030
5	0.49	0.103	0.011	0.26	0.026	0.010	0.76	0.129	0.017
6	0.59	0.136	0.036	0.17	0.024	0.023	0.76	0.160	0.030
7	0.57	0.077	0.022	0.18	0.022	0.015	0.75	0.099	0.013
8	0.68	0.051	0.030	0.18	0.045	0.031	0.86	0.096	0.030
9	0.65	0.064	0.019	0.18	0.035	0.019	0.83	0.099	0.021
10	0.60	0.092	0.009	0.23	0.035	0.009	0.83	0.127	0.010
11	0.56	0.093	0.024	0.21	0.022	0.024	0.77	0.115	0.020
12	0.56	0.071	0.008	0.20	0.020	0.006	0.76	0.091	0.011
13	0.38	0.033	0.025	0.22	0.025	0.028	0.60	0.058	0.033
14	0.29	0.045	0.023	0.16	0.012	0.023	0.45	0.057	0.025
15	0.39	0.085	0.030	0.23	0.018	0.021	0.62	0.103	0.026
16	0.51	0.072	0.017	0.17	0.022	0.016	0.68	0.094	0.018
17	0.46	0.084	0.003	0.23	0.050	0.004	0.70	0.118	0.004
18	0.52	0.088	0.012	0.28	0.040	0.014	0.80	0.128	0.013
19	0.63	0.087	0.020	0.20	0.020	0.022	0.82	0.107	0.024
20	0.43	0.088	0.018	0.37	0.065	0.017	0.80	0.153	0.025
21	0.57	0.105	0.022	0.28	0.059	0.022	0.85	0.165	0.028
22	0.33	0.068	0.008	0.33	0.052	0.014	0.66	0.121	0.018
23	0.44	0.071	0.004	0.26	0.030	0.003	0.69	0.100	0.004
24	0.50	0.064	0.028	0.12	0.016	0.030	0.62	0.080	0.030
25	0.50	0.067	0.020	0.22	0.027	0.021	0.73	0.094	0.021
26	0.60	0.081	0.020	0.26	0.040	0.022	0.86	0.121	0.024
27	0.60	0.050	0.046	0.16	0.016	0.047	0.76	0.066	0.050
28	0.47	0.050	0.005	0.24	0.017	0.005	0.71	0.067	0.006
29	0.43	0.032	0.011	0.18	0.019	0.011	0.61	0.051	0.011
30	0.73	0.093	0.074	0.18	0.045	0.282	0.92	0.138	0.338
31	0.74	0.067	0.052	0.20	0.044	0.054	0.93	0.111	0.059

$M_i = \ln(D_i+1)$, where D_i is the susceptibility deviator.
$N_i = \ln(e_i+1)$, where ϵ is the strain axis deviator.
$\sigma_{M_i} = \frac{1}{2}[\ln(D_i+1+\sigma_{D_i}) - \ln(D_i+1-\sigma_{D_i})]$.
(Susceptibility along the principal axes; $i = 1, 2, 3$).

The present work therefore provides, for the first time, a fully quantitative corelation between the magnitude of the axes of the magnetic susceptibility ellipsoid and those of the deformation ellipsoid. In so doing, the value of magnetic anisotropy as a tool for the independent investigation of natural strain in rocks is fully established.

PHILOSOPHICAL TRANSACTIONS OF THE ROYAL SOCIETY A MATHEMATICAL, PHYSICAL & ENGINEERING SCIENCES

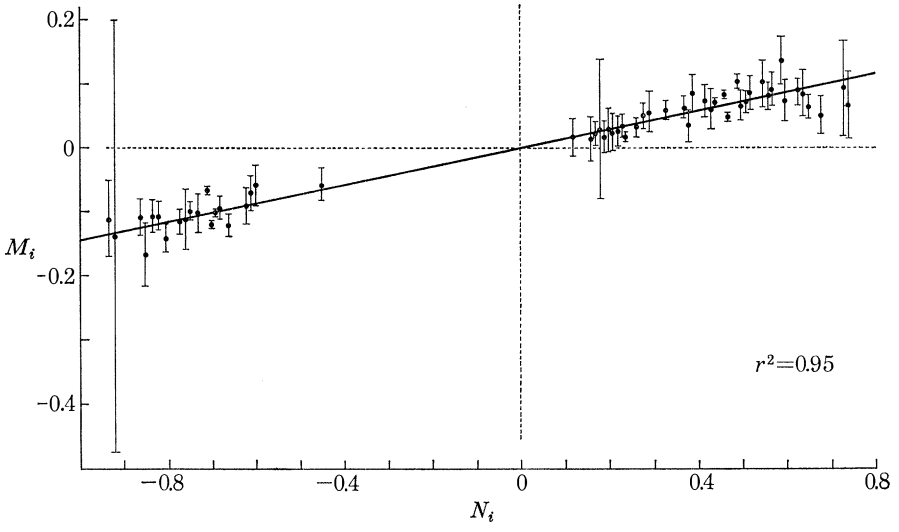

FIGURE 8. Logarithmic plot of principal normalized magnetic susceptibilities (M_i) against principal natural strains (N_i) for 31 localities in the Cambrian Slate Belt of Wales. Error bars represent standard deviations. Where several localities have the same N_i, magnetic measurements are combined into a single plot with the combined standard deviation. $M_i = 0.001 \pm 0.003 + (0.145 \pm 0.005)\ N_i$.

SEISMIC ANISOTROPY AND STRAIN

The potential value of seismic or sonic techniques in petrofabric investigation was suggested, and a method outlined by Bennett (1972). Up to the present time, there are no available data which relate seismic anisotropy to known values of finite strain. The fine-grained anisotropic aggregates afforded by the Cambrian slates of North Wales are ideal for this purpose. As an initial step in a larger programme of investigation, we have taken several samples of slate from Penrhyn Quarry at Bethesda, North Wales, and these have been independently examined at Michigan State University and at the University of Illinois. The samples are of slate with a known value of finite strain and a deformation ellipsoid with axial ratio 1.63:1:0.26. This is a reasonable average ellipsoid for the rocks in question and represents the approximate mean value of the strains shown in figure 2.

The method of investigation depends upon derivation of a simple elastic stiffness figure called the Q ellipsoid (Bennett 1972). The Q ellipsoid is a theoretical surface whose magnitude for any direction is the sum of the squares of the three seismic wave velocities for that direction. Practical determination of the Q ellipsoid depends upon measuring the velocities of the three types of body waves that can propagate through an anisotropic material. For any propagation direction, these are the pseudocompressional wave and the two orthogonally polarized pseudo shear waves. The phase velocities of these wave types are referred to as V_1, V_2 and V_3. The particle motions which correspond to these wave types form an orthogonal set with respect to the same propagation direction and the equations that relate the particle motions through the elastic stiffness coefficients were given by Cady (1946). To define the elastic or Q ellipsoid it is necessary to measure the V_1, V_2 and V_3 velocities in a minimum of six non-coplanar directions.

The orientation of the ellipsoid for any sample is controlled by the small scale shape and crystallographic elements of the rock fabric. For all anisotropic materials, the Q surface is ellipsoidal. The principal axes of the Q ellipsoid coincide with the optical indicatrix axes for

single crystals of the cubic, tetragonal, hexagonal and orthorhombic systems (Love 1927, p. 299; Cady 1946, p. 105; Kolsky 1953, p. 39; Bennett 1972). For uniaxial crystals the Q surface is an ellipsoid of revolution, and for biaxial crystals it is a triaxial ellipsoid.

If a crystal aggregate is considered as an elastic long-wave equivalent to a single crystal, then the locus of values, of which each value is the sum of the squares of the three seismic wave velocities for any particular direction, should be represented by an ellipsoidal surface. If the Q surface is ellipsoidal, then the material is homogeneous and anisotropic; the principal anisotropic directions are described by the ellipsoid axes; and the difference between the ellipsoid principal axes is a measure of the degree of elastic anisotropy.

In the present work, we have determined the V_1, V_2 and V_3 velocities in nine directions through 10 cm cube samples of slate by affixing the necessary transducers to nine pairs of randomly selected parallel surfaces cut near the margins of the initial cubic sample. The calculated value Q_i of the Q ellipsoid for the ith direction is given by:

$$Q_i = Q_i'/\rho = (V_1^2 + V_2^2 + V_3^2)_i$$

where ρ is the density, V_i is the P wave velocity for the ith direction, and V_2 and V_3 are the velocities of the two orthogonally polarized shear waves for the ith direction.

TABLE 3. SEISMIC VELOCITIES FOR AN AVERAGE FINITE STRAIN STATE OF THE CAMBRIAN SLATE BELT OF WALES. ($\epsilon_1 = 1.20$; $\epsilon_2 = 0.33$; $\epsilon_3 = -0.65$)

wave type	propagation direction	vibration direction	symbol	velocity/(km/s)			
P	X	—	(P_X)	6.555	6.552	6.596	6.591
P	Y	—	(P_Y)	6.194	6.125	6.126	6.143
P	Z	—	(P_Z)	5.228	5.229	5.303	5.290
S	X	Y	(S_{x_y})	3.775	3.816		
S	X	Z	(S_{x_z})	2.835	2.881		
S	Y	X	(S_{y_x})	3.796	3.841		
S	Y	Z	(S_{y_z})	2.867	2.887		
S	Z	X	(S_{z_x})	2.856	2.869		
S	Z	Y	(S_{z_y})	2.880	2.897		

Average deformation ellipsoid 1.63:1:0.26
Average Q ellipsoid 1.10:1:0.73

By defining the polarization plane as the plane that contains the propagation direction and shear wave particle motion, the two polarization planes are virtually orthogonal for any propagation direction and the values of V_2 and V_3 can usually be measured unambiguously for any particular direction (Tilmann & Bennett 1973*a*). Since the density term is constant, it may be incorporated into the Q_i' term without affecting the shape or orientation of the Q ellipsoid. The details of the method are given by Tilmann & Bennett (1973*b*). It involves calculation of the least squares value of the Q ellipsoid for all directions and enables the principal axes of the Q ellipsoid to be obtained using the method of successive approximation (Nye 1957).

The principal axes of the ellipsoid are found to coincide precisely with the principal strain directions, thereby demonstrating the almost perfect orthorhombic symmetry of the rocks in question. The measured velocities were found to be very closely reproducible and representative values are given in table 3. The pseudocompressional and pseudo shear waves are termed P and S respectively, with the suffix (X, Y, Z) referring to the direction of propagation, and the econd suffix (x, y, z) in the case of the shear waves referring to the direction of particle m otion.

Thus $S_{X,y}$ is the pseudo shear wave propagating parallel to X and vibrating parallel to Y. For convenience, the average wave velocities in the principal directions are shown schematically in figure 9, plate 1. The higher velocities of P waves in the cleavage plane are to be expected. These are such that the P wave velocity in the X direction (6.55 km/s) is 26 % higher than the Z direction (5.2 km/s) and the P wave velocity in the Y direction is 18 % higher than in the Z direction, whereas the P wave velocity in the X direction is only 6.5 % higher than in the Y direction. The effect of the anisotropy provided by the cleavage is even more apparent from the S waves. Those propagating across the cleavage have low and similar velocities ($S_{Z,x}$ and $S_{Z,y}$), whereas the shear waves that propagate and vibrate within the cleavage ($S_{X,y}$ and $S_{Y,x}$) are appreciably higher. $S_{X,y}$ has a 30 % higher velocity than $S_{X,z}$ and $S_{Y,x}$ has a 32 % higher velocity than $S_{Y,z}$. It is of interest to note that the two similar velocity shear waves propagating parallel to Z ($S_{Z,x}$ and $S_{Z,y}$) also have almost the same velocity as those shear waves which have Z as their vibration direction ($S_{X,z}$ and $S_{Y,z}$). For a uniform aggregate $S_{Z,x}$ and $S_{X,z}$ should be equal; $S_{Z,y}$ and $S_{Y,z}$ should be equal; and $S_{X,y}$ and $S_{Y,x}$ should be equal. The fact that two of these pairs are virtually identical and the third is close, reflects a high degree of uniformity in the material.

The measurements obtained demonstrate that whereas the individual silicate crystals of the rock do not possess a centre of symmetry, the rock as a whole does, and behaves as a pseudo single crystal of higher than monoclinic symmetry. The extent of the difference in P wave velocities for different directions and the degree of birefringence of orthogonally polarized shear waves for a single propagation direction are considerable. For the average finite strain state of the Welsh Cambrian Slate Belt, with a deformation ellipsoid of form 1.63:1:0.26, the elastic or Q ellipsoid has principal axes in the ratio 1.10:1:0.73. The variations in seismic velocity for difierent principal strain directions are such that it will be possible to establish the nature of systematic changes in velocity as a function of variations in finite state of strain.

References (Wood *et al.*)

Anderson, P. W., Merritt, F. R., Remika, J. P. & Yager, W. A. 1954 *Phys. Rev.* **93**, 717–718.
Baker, D. W., Wenk, H. R. & Christie, J. M. 1969 *J. Geol.* **77**, 144–172.
Bennett, H. F. 1972 *J. geophys. Res.* **77**, 3078–3080.
Cady, W. G. 1946 *Piezoelectricity*. New York: McGraw-Hill.
Collinson, D. W., Molyneux, L. & Stone, D. B. 1963 *J. scient. Instrum.* **40**, 310–312.
Fisher, R. A. 1953 *Proc. R. Soc. Lond.* A **217**, 295–305.
Fuller, M. D. 1960 *Nature, Lond.* **186**, 791–792.
Fuller, M. D. 1963 *J. geophys. Res.* **68**, 293–309.
Fuller, M. D. 1964 *J. Geol.* **72**, 368–376.
Graham, J. W. 1954 *Bull. geol. Soc. Am.* **65**, 1257–1258.
Kolsky, H. 1953 *Stress waves in solids*. Oxford at the Clarendon Press, London.
Kumagai, H., Abe, H., Ono, K., Hayashi, I., Shimada, J. & Iwanaga, K. 1955 *Phys. Rev.* **99**, 1116–1118.
Love, A. E. H. 1927 *A treatise on the mathematical theory of elasticity*. Cambridge University Press.
March, A. 1932 *Zeitschr. Kristallogr.* **81**, 285–297.
Means, W. D. & Paterson, M. S. 1966 *Beitr. Mineral. Petrogr.* **13**, 108–133.
Mizushima, K. & Iida, S. 1966 *J. Phys. Soc. Jap.* **21**, 1521–1526.
Molyneux, L. 1971 *Geophys. J. R. astr. Soc.* **24**, 429–433.
Nye, J. F. 1957 *Physical properties of crystals*. Oxford at the Clarendon Press, London.
Oertel, G. 1970 *Bull. geol. Soc. Am.* **81**, 1173–1188.
Oertel, G. & Curtis, C. D. 1972 *Bull. geol. Soc. Am.* **83**, 2597–2606.
Oertel, G. & Wood, D. S. 1974 *Trans. Am. Geophys. Union* **55** (7), 695.
Owens, W. H. 1973 *Tectonophysics* **16**, 249–261.
Porath, M. 1968 *Phil. Mag.* **17**, 602–608.
Ramsay, J. G. & Wood, D. S. 1973 *Tectonophysics* **16**, 263–277.

PHILOSOPHICAL TRANSACTIONS OF THE ROYAL SOCIETY A MATHEMATICAL, PHYSICAL & ENGINEERING SCIENCES

Sander, B. & Sachs, B. 1930 *Zeitschr. Kristallogr.* **75**, 529–540.
Singh, J., Sanderson, D. J. & Tarling, D. H. 1975 *Tectonophysics* **27**, 141–153.
Sorby, H. C. 1855 *Phil. Mag.* **11**, 20–37.
Starkey, J. 1964 *Am. J. Sci.* **262**, 735–752.
Tasaki, A. & Iida, S. 1963 *J. Phys. Soc. Jap.* **18**, 1148–1154.
Tilmann, S. E. & Bennett, H. F. 1973*a* *J. geophys. Res.* **78**, 7623–7629.
Tilmann, S. E. & Bennett, H. F. 1973*b* *J. geophys. Res.* **78**, 8463–8469.
Tullis, T. E. 1971 Unpublished Ph.D. thesis, University of California, Los Angeles.
Tullis, T. E. & Wood, D. S. 1972 *Geol. Soc. Am.* (Abstr. with programs, **4** (7), 694.
Tullis, T. E. & Wood, D. S. 1975 *Bull. geol. Soc. Am.* **86**, 632–638.
Wenk, H. R. 1963 *Schwiez. Mineral. Petrogr. Mitt.* **43**, 709–719.
Wenk, H. R. 1965 *Schweiz. Mineral. Petrogr. Mitt.* **45**, 517–550.
Wood, D. S. 1974 *Ann. Rev. Earth and Plan. Sci.* **2**, 369–401.

Discussion

D. H. Tarling (*Department of Geophysics and Planetary Physics, The University, Newcastle upon Tyne, NE*1 7*RU*). The magnetic fabric of a rock is highly sensitive to slight changes in grain shape of the ferromagnetic minerals that may arise from low stress fields being applied to undeformed rocks. This technique is therefore ideally suited for determining such strain changes in low stress environments, but is somewhat insensitive for grain-shape alterations as a result of an increase from moderate to high strain. In the Cambrian Slate Belt, the strain deformation is high so that the magnetic fabric is unlikely to be a good indicator of the magnitude of strain. It does, however, provide an extremely rapid tool for determining the gross fabric and particularly the direction of the net total strain to which the fabric has been subjected.

PHILOSOPHICAL TRANSACTIONS OF THE ROYAL SOCIETY A MATHEMATICAL, PHYSICAL & ENGINEERING SCIENCES

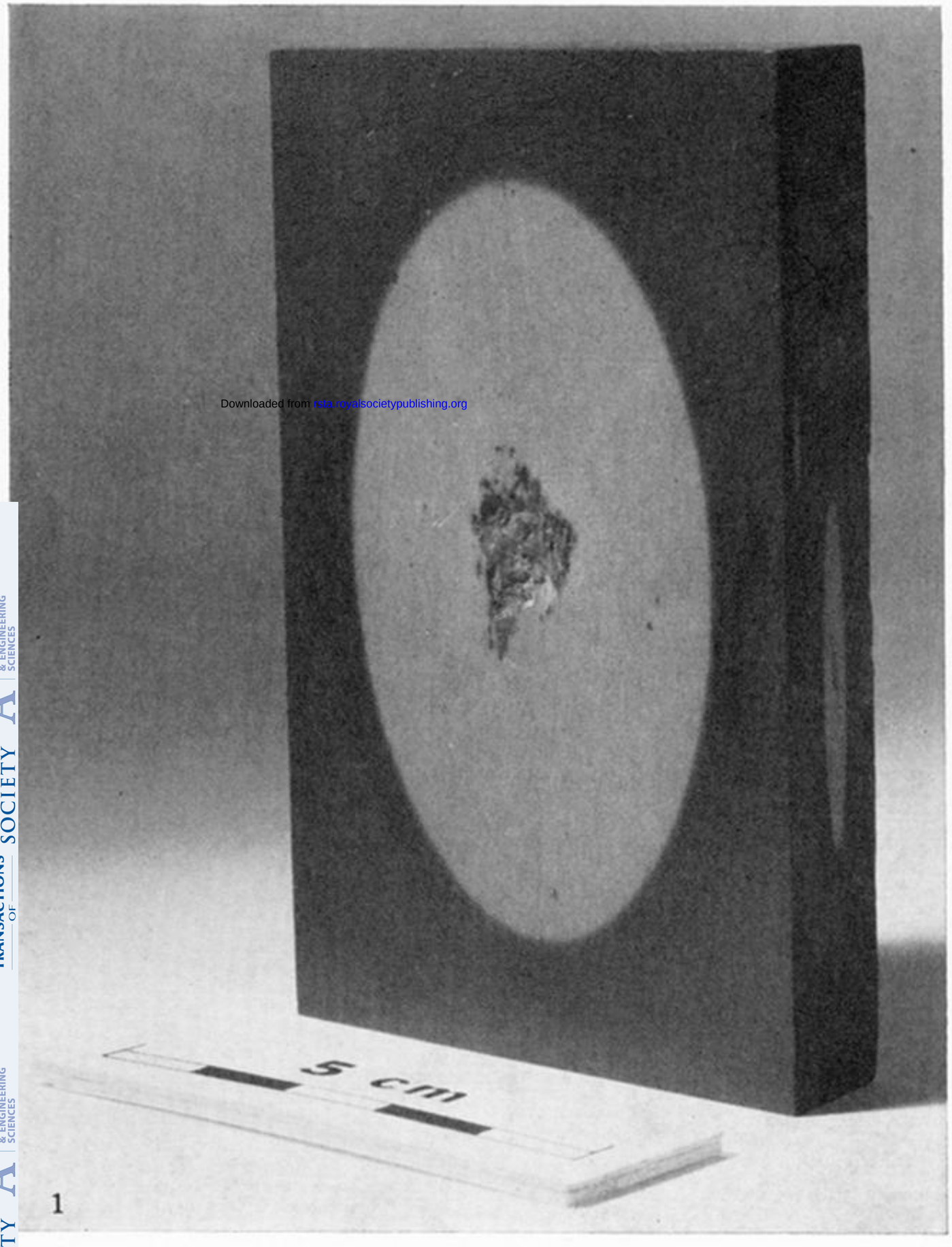

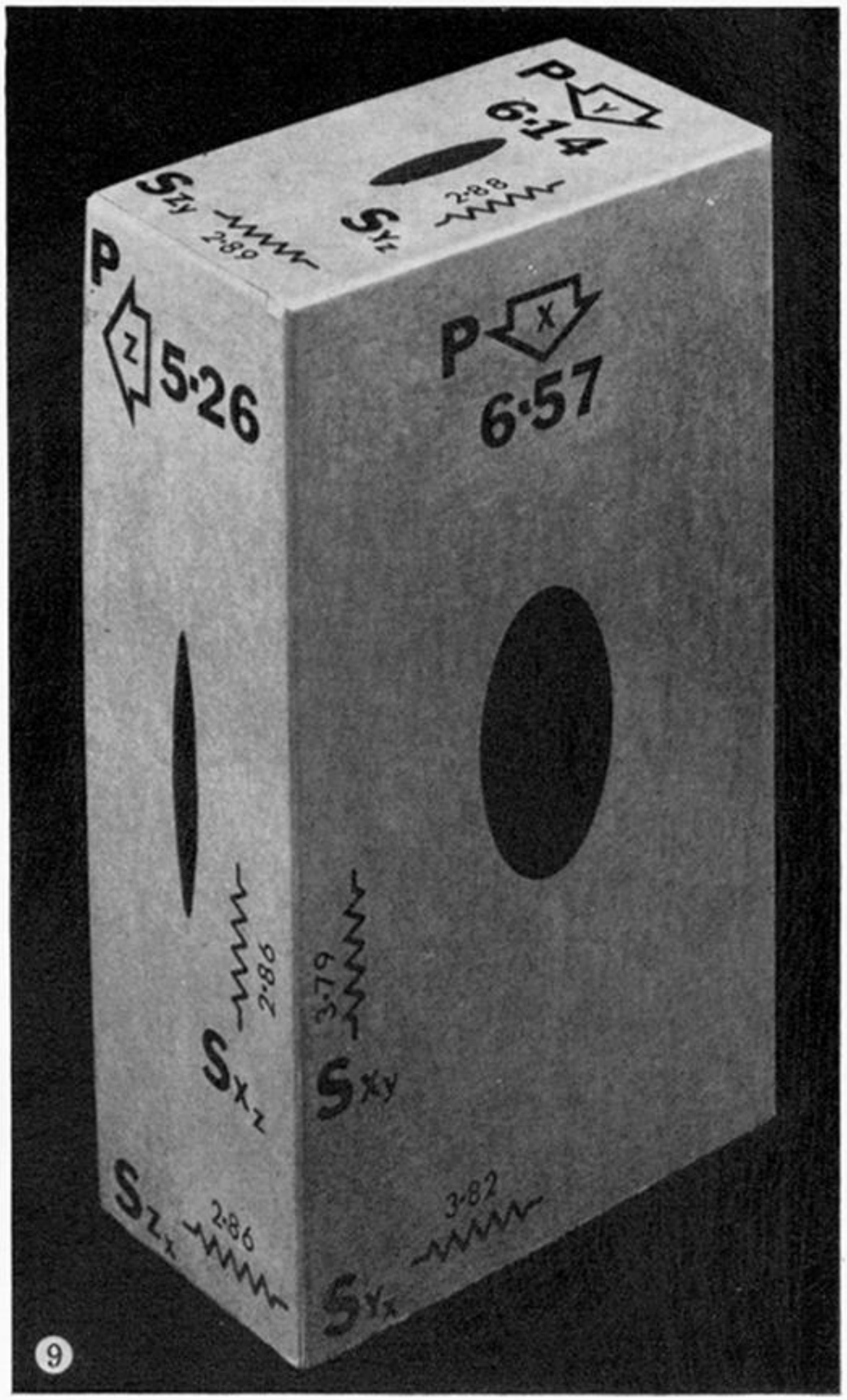

FIGURE 1. Ellipsoidal iron-reduction bodies from the Lower Cambrian slates at Penrhyn Quarry, Bethesda, North Wales. Specimen cut parallel and perpendicular to the cleavage showing the principal plane (X–Y) and the plane X–Z of the deformation ellipsoid.

FIGURE 9. Schematic block representation of the 9 seismic velocities for the principal strain directions X, Y and Z of slate with deformation ellipsoid of axial ratio 1.63:1:0.26 from Penrhyn Quarry, Bethesda, North Wales. Arrows indicate propagation direction of P waves. Propagation and vibration directions of S waves indicated. Velocities are in kilometres per second.